Imaging Properties of Kinoform Fibonacci Lenses
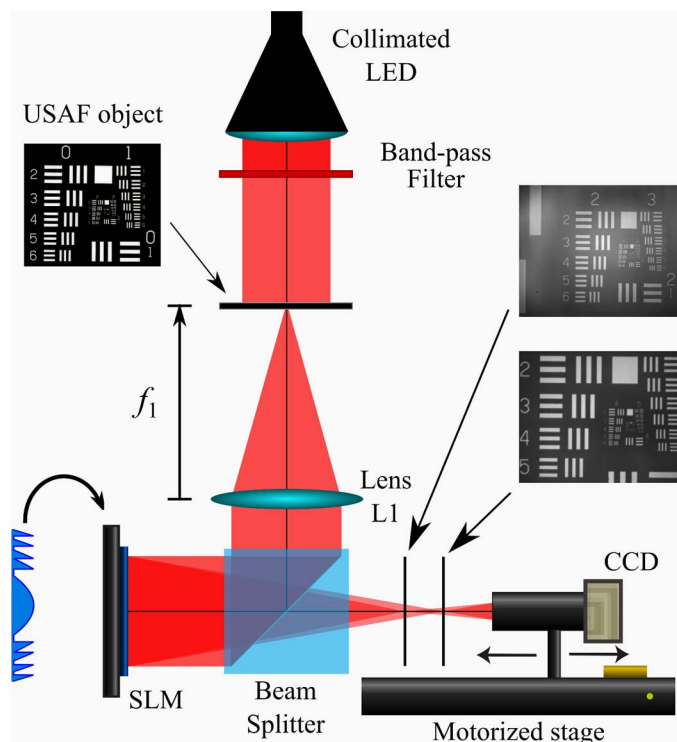
V. Ferrando
A. Calatayud
P. Andrés
R. Torroba
W. D. Furlan
J. A. Monsoriu

Imaging Properties of Kinoform Fibonacci Lenses

V. Ferrando,[1,2] **A. Calatayud,**[1] **P. Andrés,**[2] **R. Torroba,**[3] **W. D. Furlan,**[2] **and J. A. Monsoriu**[1]

[1]Centro de Tecnologías Físicas, Universitat Politècnica de València, E-46022 Valencia, Spain
[2]Departamento de Óptica, Universitat de València, E-46100 Burjassot, Spain
[3]Centro de Investigaciones Ópticas (CONICET La Plata-CIC) and UID OPTIMO, Facultad de Ingeniería, Universidad Nacional de La Plata, C.P 1897, La Plata, Argentina

Abstract: In this paper, we present a new kind of bifocal kinoform lenses in which the phase distribution is based on the Fibonacci sequence. The focusing properties of these DOEs coined Kinoform Fibonacci lenses (KFLs) are analytically studied and compared with binary-phase Fibonacci lenses (FLs). It is shown that, under monochromatic illumination, a KFL drives most of the incoming light into two single foci, improving in this way the efficiency of the FLs. We have also implemented these lenses with a spatial light modulator. The first images obtained with this type of lenses are presented and evaluated.

Index Terms: Fibonacci, diffraction, kinoform lens.

1. Introduction

Over the last decades the role of aperiodic order (order without periodicity [1]) in nature has been deserved a growing interest by the scientific community. In fact, the observation of nature has allowed scientists to perceive different kinds of morphological orders, being the Fibonacci sequence, one of the most recurrent mathematical fitting models. It is well known that the ratio of two consecutive elements of the Fibonacci sequence approaches asymptotically an irrational number known as the golden mean and that this number is frequently associated with some subjective concepts such as equilibrium, or harmony. Fibonacci series and the golden mean can be found profusely in nature, from the helical arrangement of seeds and leaves of plants [2] to all dynamical systems exhibiting the period-doubling route to chaos [3]. Artificial Fibonacci patterns also appear on core/shell structures constructed through stress-driven self assembly induced by cooling [4], and the golden mean has recently been found in the fine structure of spin dynamics around critical points in quantum phase transitions [5], just to name a few. Photonics is a potential field of applications for novel devices designed and constructed using the Fibonacci sequence [6]. Supported in part by the enormous progress in technology development in this area, quantum cascade lasers based on a Fibonacci distributed feedback sequence [7], and Fibonacci arrays of
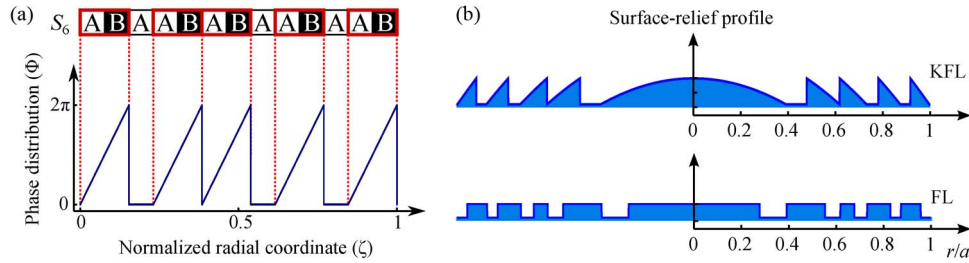
Fig. 1. (a) Phase profile of the S_6 based KFL represented against a squared radial coordinate. (b) KFL and FL surface-relief profiles generated from a Fibonacci sequence of order $j = 6$.

nanoparticles that produce quasi-periodic distribution of plasmon modes [8], have been recently proposed. Following this trend, our group has recently proposed the Fibonacci Lenses (FLs) [9], which are diffractive lenses constructed using the Fibonacci sequence.

A FL is a binary lens that, like a conventional Fresnel zone plate, produces intensity maxima along the optical axis at odd fractions of its main focal distance. However, in this case each focus is axially doubled. These twin foci are located one in front and one behind the focus of an equivalent Fresnel zone plate of the same number of zones. The axial positions of this foci are given by the Fibonacci numbers, being the golden mean the ratio of the two FL focal distances. Moreover, we found that the golden mean is also the responsible of the energetic balance of both foci and also of their axial and transverse resolution. Inspired on FLs we recently proposed a new type of bifocal vortex lenses, the Fibonacci Vortex Lenses (FVLs) [10], that produce a twin optical vortices along the axial coordinate. The positions of these vortices depend on the two incommensurable periods of the Fibonacci sequence in which the FVL is based on. The radii of these twin vortices increase with the topological charge of the vortex lens and their ratio is the golden mean. Although the binary FL and FVL are effective in controlling the luminous intensity, their diffraction efficiency is relatively low.

Since the diffraction efficiency of Diffractive Optical Elements (DOEs) is crucial for certain practical applications, in this work we introduce the concept of Kinoform Fibonacci Lenses (KFLs), i.e., blazed zone plates with a radial structure based on the Fibonacci sequence. KFLs design is formally presented in this paper and an analytical expression for the phase profile is derived. As blazed DOEs, KFLs drive most of the incoming light into a splitted main focus, improving in this way the efficiency of FLs. This fact is demonstrated theoretically by means of the Modulation Transfer Function (MTF) and experimentally in an image forming experiment.

2. Kinoform Fibonacci Lenses Design

A KFL is defined as a pure phase diffractive element whose radial phase distribution is obtained from the Fibonacci sequence as follows: Starting with two elements (seeds) $F_0 = 0$ and $F_1 = 1$, the Fibonacci numbers, $F_j = \{0, 1, 1, 2, 3, 5, 8, 13, 21, \ldots\}$, are obtained by the sequential application of the iterative rule $F_{j+1} = F_j + F_{j-1}$, $(j = 1, 2, \ldots)$. The golden mean, or golden ratio, is defined as the limit of two consecutive Fibonacci numbers: $\varphi = \lim_{j \to \infty} F_j/F_{j-1} = (1 + \sqrt{5})/2$.

In a similar way, a binary aperiodic Fibonacci sequence can also be deterministically generated with two seed elements, as for exemple, $S_1 = \{A\}$ and $S_0 = \{B\}$ and the succesive elements of the sequence are obtained simply as the concatenation of the two previous ones: $S_{j+1} = \{S_j \, S_{j-1}\}$ for $j \geq 1$. In this way, $S_2 = \{AB\}$, $S_3 = \{ABA\}$, $S_4 = \{ABAAB\}$, $S_5 = \{ABAABABA\}$, and so on. Note that, in any given sequence of order S_j, two succesive "B" are separated by either, one or two "A", and that the total number of elements F_{j+1}, results from the sum of F_j elements "A", and F_{j-1} elements "B". In the design of a KFL each element of the Fibonacci sequence can be used to define the generating function, $\Phi(\zeta)$, for the radial phase distribution of the lens: With compact support in the interval [0, 1], $\Phi(\zeta)$ is defined with a linear variation between $\Phi = 0$ and $\Phi = 2\pi$ at

each subinterval $\{AB\}$ of the sequence, being $\Phi = 0$ otherwise [see Fig. 1(a)]. Thus, the generating function of the radial phase for the jth order KFL can be written analytically as

$$\Phi_j^{KFL}(\zeta) = -\frac{2\pi}{2d_j} \sum_{i=1}^{F_{j-1}} \text{rect}\left(\frac{\zeta - \zeta_{i,j}}{2d_j}\right)(d_j + \zeta_{i,j} - \zeta) \tag{1}$$

where $d_j = 1/F_{j+1}$, $\zeta = r^2/a^2$ is the normalized radial coordinate, and $\zeta_{i,j}$ is the position for the ith element "B" of the sequence. This position can be obtained as $\zeta_{i,j} = (\lfloor(\varphi + 1)i\rfloor - 1) \cdot d_j$, being $\lfloor x \rfloor$ the floor function of x [11]. For example, applying Eq. (1), the generating function of the radial phase for $j = 6$ order is given by:

$$\Phi_6^{KFL}(\zeta) = -\pi(2 - 13\zeta)\text{rect}\left[\frac{(\zeta - 1/13)}{2/13}\right] - \pi(5 - 13\zeta)\text{rect}\left[\frac{(\zeta - 4/13)}{2/13}\right]$$
$$-\pi(7 - 13\zeta)\text{rect}\left[\frac{(\zeta - 6/13)}{2/13}\right] - \pi(10 - 13\zeta)\text{rect}\left[\frac{(\zeta - 9/13)}{2/13}\right] - \pi(13 - 13\zeta)\text{rect}\left[\frac{(\zeta - 12/13)}{2/13}\right]. \tag{2}$$

The profile of the KFL generated by Eq. (2) is represented in Fig. 1(b). For comparison the radial profile of a FL of the same focal distance is represented in the same figure. As can be seen obtaining the phase of a KFL from the phase of FL is not a trivial task as it is for a Kinoform Fresnel lens from a binary-phase Fresnel lens. As it was not previously reported, the generating function of the radial phase corresponding to a FL, Φ_j^{FL}, is defined here for completeness:

$$\Phi_j^{FL}(\zeta) = \pi \sum_{i=1}^{F_{j-1}} \text{rect}\left(\frac{\zeta - \zeta_{i,j} - \frac{d_j}{2}}{d_j}\right). \tag{3}$$

3. Focusing and Imaging Properties

To evaluate the focusing properties of the KFLs it is of interest to compute the axial irradiance provided by these lenses normally illuminated by a plane wave of wavelength λ. Within the Fresnel aproximation the axial irradiance function is given by

$$I(u) = 4\pi u^2 \left| \int_0^1 t(\zeta)\exp(-2\pi i u\zeta)\, d\zeta \right|^2 \tag{4}$$

where $u = a^2/2\lambda z$ is the reduced axial coordinate, a is the lens radi, $t(\zeta) = \exp[i\Phi(\zeta)]$ is the transmitance function, being $\Phi_j(\zeta)$ the phase of the lens. By using the Eq. (4) we have computed the axial irradiances provided by KFLs of order S_8 and S_{10} and for comparison pourposes those corresponding to FLs of the same orders. The results are shown in Fig. 2.

As can be seen the KFLs drive most of the incoming light into two single foci located at $u_1 \simeq F_{j-1}$ and $u_2 \simeq F_j$, being the ratio of the focal distances $u_2/u_1 \simeq \varphi$. On the other hand, as shown in [9], FLs provide multiple diffraction orders due to the binary nature of the structure. Each order presents two diffraction peaks, due to its quasiperiodic distribution of zones with two inconmensurable periods. The first order foci of the FL coincide with the foci of the KFL, but their relative intensity is 60% lower.

The performance of a KFL as an image forming device is analyzed in the spatial-frequency domain by calculation of the MTFs at the two focal planes (see Fig. 3). To that end, a MATLAB algorithm has been employed for numerically evaluating the autocorrelation function of the generalized pupil function represented in a 1001×1001 matrix. As can be seen, in a similar fashion to the effect of the kinoform profile on the axial irradiance, the MTFs reveal the improved performance of a KFL provided by the blazed profile, especially in the mid-low range of frequencies.

We have experimentally tested the imaging capabilities of KFLs and FLs of the same main focal distances. A schematic illustration of the experimental setup if shown in Fig. 4(a). The diffractive lenses were implemented on a Liquid Crystal in a Silicon SLM (Holoeye PLUTO, 8-bit gray-level,
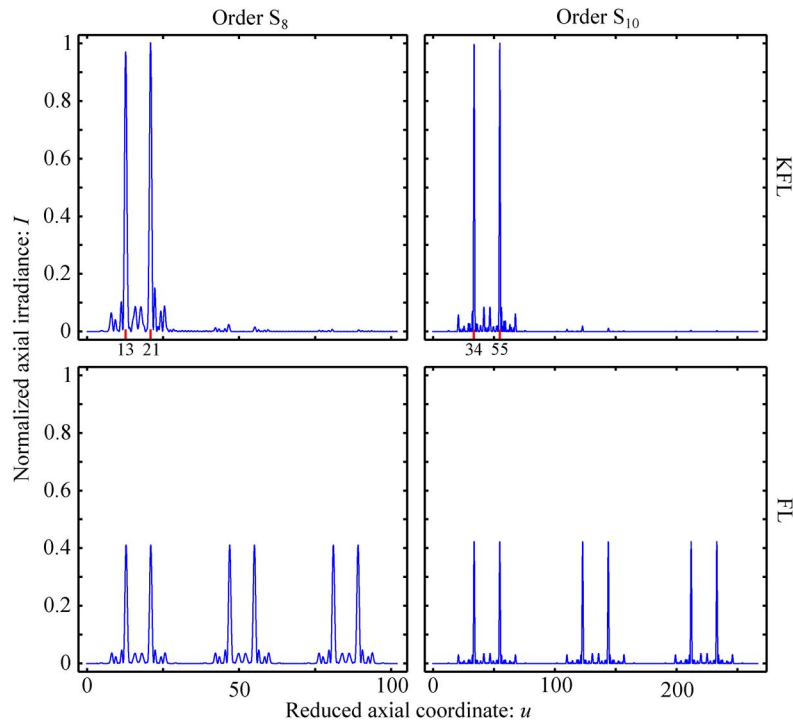
Fig. 2. Normalized axial irradiances provided by FLs and KFLs of orders S_8 and S_{10}.
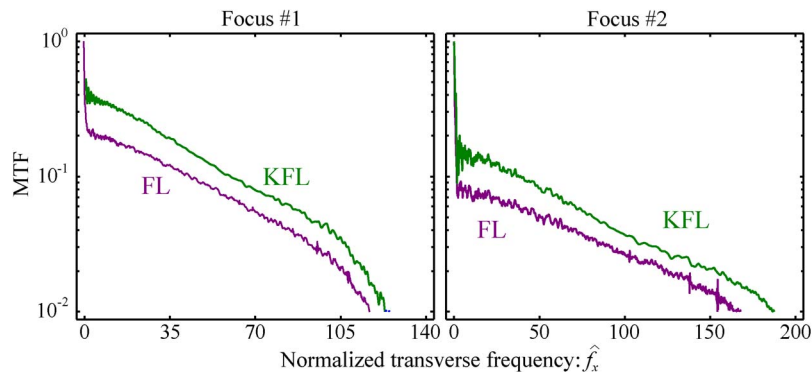

Fig. 3. MTFs at both foci of KFL and FL of the same order (S_{10}).

pixel size 8 μm, and resolution 1920 $\times$ 1080 pixels), calibrated for a 2π phase shift at $\lambda = 633$ nm and operating in phase-only modulation mode. The illumination system consists of a red collimated LED (Mounted High-Power LED, red 625 nm, 1000 mA) and a bandpass filter ($\lambda = 632.8 \pm 0.6$ nm). A test object (the 1951 USAF resolution test chart) was mounted at the focal plane of achromatic Badal Lens, L_1, (focal length: 160 mm). The images produced by the diffractive lenses were captured and registered with a CCD camera (8 bit gray-level, pixel pitch of 3.75 μm, and 1280 $\times$ 960 pixels) mounted on a translation stage (Thorlabs LTS 300; range: 300 mm; precision: 5 μm) along the optical axis. The images produced by a KFL and a FL at both focal planes are shown in Fig. 4(b). A profile of the irradiance, measured along a single element of the image of the test is shown in Fig. 4(c). As can be seen, the images provided by the KFL have higher contrast, C, than those provided by the FL of the same order ($C_{FL}/C_{KFL} \approx 0.6641$). On the other hand it can be observed that, as expected, the relative size of the images at both planes also are related by the golden ratio. In fact in Fig. 4(b) the relative sizes of the segments a and b satisfy $a/b \approx \varphi$.
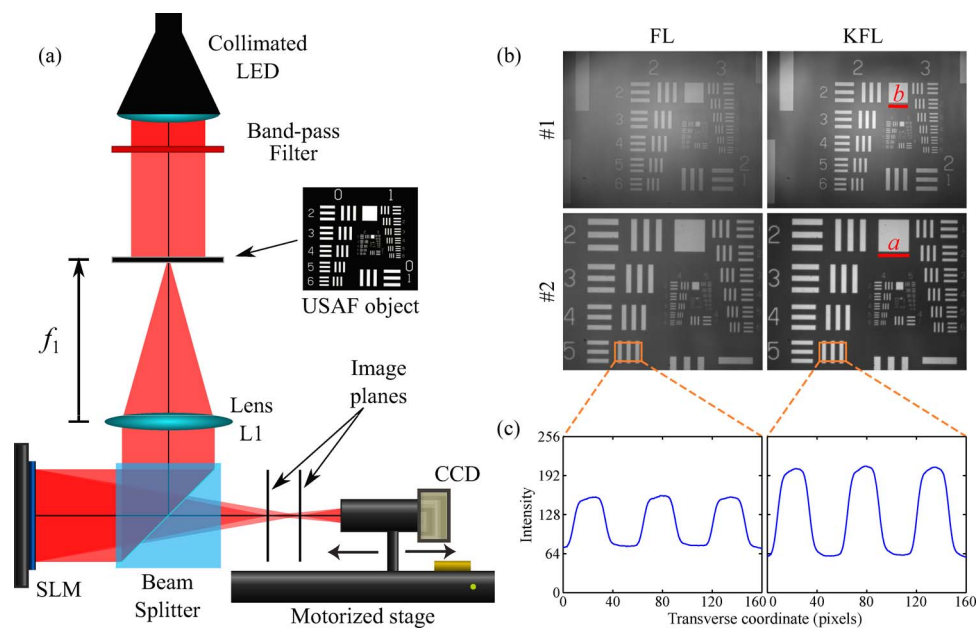
Fig. 4. (a) Experimental setup employed for recording the images produced by KFLs and FLs. (b) Images of the USAF object produced by a KFL and a FL of order S_{10} at focus #1 and focus #2. (c) Profiles of the irradiances obtained at focus #2 of both for the vertical 2–4 group images.

4. Conclusion

We have presented a novel design of Fibonacci lenses with improved focusing and imaging capabilities. These lenses have a blazed profile whose analytical expression has been deduced. KFLs present two single foci, being the golden mean, the ratio of the two focal distances. The higher quality of the images produced by KFLs are demonstrated theoretically and experimentally. On the one hand, the MTFs obtained for KFLs display superior performance over the MTFs obtained for FLs. Moreover, the first images produced by these kind of lenses are reported. Due to their exclusive properties, we believe that KFLs could be of benefit in several potential applications for instance, in optical trapping, in optical micromachining, and in confocal microscopy. In particular, we suggest that the bifocal structure of a KFL can find applications in Ophthalmology to design intraocular or contact lenses for the correction of presbyopia. Additionally, the concept of FKL can be easily extended to other geometries, like square zone plates [12]. For different applications further resolution improvements can be obtained by using higher Fibonacci orders in the lens design and/or by combining two or more Fibonacci orders in a single lens [13].

References

[1] E. Maciá, "The role of aperiodic order in science and technology," *Rep. Prog. Phys.*, vol. 69, no. 2, pp. 397–441, Feb. 2006.
[2] A. J. Fleming, "Plant mathematics and Fibonacci's flowers," *Nature*, vol. 418, no. 6899, p. 723, Aug. 2002.
[3] G. Linage, F. Montoya, A. Sarmiento, K. Showalter, and P. Parmananda, "Fibonacci order in the period-doubling cascade to chaos," *Phys. Lett. A*, vol. 359, no. 6, pp. 638–639, Dec. 2006.
[4] C. Li, X. Zhang, and Z. Cao, "Triangular and Fibonacci number patterns driven by stress on core/shell microstructures," *Science*, vol. 309, no. 5736, pp. 909–911, Aug. 2005.
[5] R. Coldea, D. A. Tennant, E. M. Wheeler, E. Wawrzynska, D. Prabhakaran, M. Telling, K. Habicht, P. Smeibidl, and K. Kiefer, "Quantum criticality in an Ising chain: Experimental evidence for emergent E8 symmetry," *Science*, vol. 327, no. 5962, pp. 177–180, Jan. 2010.
[6] E. Maciá, "Exploiting aperiodic designs in nanophotonic devices," *Rep. Prog. Phys.*, vol. 75, no. 3, p. 036502, Mar. 2012.
[7] L. Mahler, A. Tredicucci, F. Beltram, C. Walther, J. Faist, H. E. Beere, D. A. Ritchie, and D. S. Wiersma, "Quasi-periodic distributed feedback laser," *Nat. Photon.*, vol. 4, no. 3, pp. 165–169, Jan. 2010.

[8] R. Dallapiccola, A. Gopinath, F. Stellacci, and L. Dal Negro, "Quasi-periodic distribution of plasmon modes in two-dimensional Fibonacci arrays of metal nanoparticles," *Opt. Exp.*, vol. 16, no. 8, pp. 5544–5555, Apr. 2008.

[9] J. A. Monsoriu, A. Calatayud, L. Remón, W. D. Furlan, G. Saavedra, and P. Andrés, "Bifocal Fibonacci diffractive lenses," *IEEE Photon. J.*, vol. 5, no. 3, p. 3400106, Jun. 2013.

[10] A. Calatayud, V. Ferrando, L. Remón, W. D. Furlan, and J. A. Monsoriu, "Twin axial vortices generated by Fibonacci lenses," *Opt. Exp.*, vol. 21, no. 8, pp. 10 234–10 239, Apr. 2013.

[11] K. Redish and W. Smyth, "Closed form expressions for the iterated floor function," *Discrete Math.*, vol. 91, no. 3, pp. 317–321, Sep. 1990.

[12] A. Calatayud, V. Ferrando, F. Giménez, W. D. Furlan, G. Saavedra, and J. A. Monsoriu, "Fractal square zone plates," *Opt. Commun.*, vol. 286, no. 1, pp. 42–45, Sep. 2013.

[13] F. Giménez, W. D. Furlan, A. Calatayud, and J. A. Monsoriu, "Multifractal zone plates," *J. Opt. Soc. Amer. A*, vol. 27, no. 8, p. 1851, Jul. 2010.